Electronic properties of polyacetylene prepared by the Durham 'photoisomer' route

C. A. Jones*, R. A. Lawrence, J. Martens and R. H. Friend†
Cavendish Laboratory, Madingley Road, Cambridge, CB3 0HE, UK

and D. Parker and W. J. Feast
Department of Chemistry and Interdisciplinary Research Centre in Polymer Science and Technology, University of Durham, Durham DH1 3LE, UK

and M. Lögdlund and W. R. Salaneck
Linköping Institute of Technology, Department of Physics and Measurement Technology, S-58183 Linköping, Sweden
(Received 17 September 1990; accepted 22 November 1990)

We report here the properties of polyacetylene prepared via a precursor polymer, modified from the standard Durham precursor by photoisomerization of the monomer to 3,6-bis(trifluoromethyl)pentacyclo-[6.2.0.0^{2,4},O^{3,6},O^{5,7}]dec-9-ene. This modification gives a precursor with improved thermal stability, in that conversion to polyacetylene only occurs above 60°C. The conversion is highly exothermic, but the method is suitable for the formation of thin films. There is evidence from infra-red and X-ray photoelectron spectroscopy measurements for retention of fluorine in the thermally treated polymer, and we consider that this is probably due to isomerization of some of the side groups on the precursor polymer, rather than their elimination. Polyacetylene produced in the form of thin unoriented films is highly disordered, with a coherence length interchain order determined from X-ray scattering of only 1.8 nm. The electronic and vibrational structure of these films is much affected by the disorder, with the peak in the π–π^* optical absorption band at 2.65 eV, and correspondingly high Raman-active vibrational modes. We compare also the properties of polymers prepared with different degrees of polymerization, achieved by addition of a chain transfer agent during polymerization of the monomer to form the precursor polymer. There is some evidence from the Raman spectra that the lower molecular weight precursors produce better ordered polyacetylene.

(Keywords: polyacetylene; photoisomerization; Durham route)

INTRODUCTION

Precursor routes to conjugated polymers

The use of precursor polymer routes to conjugated polymers which are themselves intractable has been widely developed over the past decade. The goal is to be able to process the precursor polymer, usually in solution, and to convert to the final conjugated polymer *in situ* by a thermal elimination reaction. This was first developed with polyacetylene using the 'Durham' precursor route shown as A, B, C and D-PA in *Figure 1*[1]. The precursor polymer, B, is readily handled in solvents such as butanone, and polyacetylene films of very high quality can be obtained. These have recently been used for the construction of semiconductor devices including metal insulator semiconductor field effect transistors (MISFETs)[2]. The kinetics of the transformation and *cis–trans* isomerization reactions have been extensively studied[3,4], and the various steps are well understood. Though this route is very convenient, the precursor polymer is not stable at room temperature, as the elimination to form polyacetylene is a symmetry-allowed reaction, and the polymer must be stored at low temperatures.

An alternative route (A, D, E, D-PA in *Figure 1*) was first demonstrated by Feast and Winter[5]. In this approach, A is first converted to its photoisomer, D, 3,6-bis(trifluoromethyl) pentacyclo[6.2.0.0^{2,4},O^{3,6},O^{5,7}]dec-9-ene, which gives the precursor polymer E on ring-opening metathesis polymerization. The anticipated

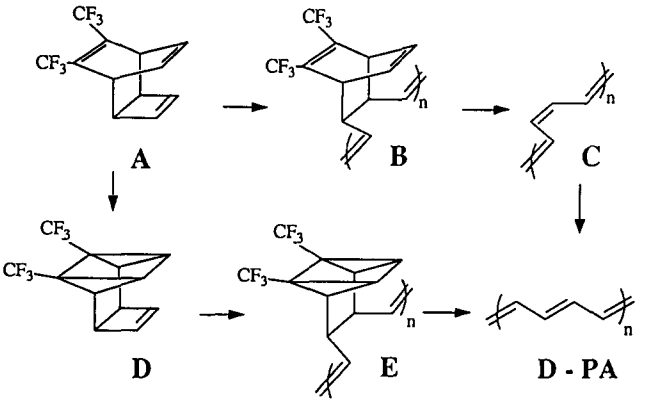

Figure 1 Synthetic routes to polyacetylene: A, B, C, F is the standard Durham route[1]; A, D, E is the 'photoisomer' route[5]

* Current address: British Telecom Research Laboratories, Martlesham Heath, Ipswich IP5 7RE, UK
† To whom correspondence should be addressed

0032-3861/91/071200-10

advantage here is that the conversion of the precursor polymer to polyacetylene is no longer symmetry-allowed so that the precursor is much more stable thermally, requiring temperatures in excess of 60°C to bring about conversion. In practice polyacetylene films are usually generated between 100°C and 120°C. The disadvantage is that the elimination reaction is strongly exothermic[6] and there is risk of thermal runaway (or explosion) if bulk samples or thick films are converted. Dilute solutions and thin films of the precursor however, can be handled safely, and we report here a survey of structural and electronic properties of the polyacetylene prepared in this way. We have compared the properties of polyacetylene films of different molecular weights, obtained by the use of a chain transfer agent in the precursor polymer synthesis.

Polyacetylene prepared via the standard Durham precursor route is known to have a very poorly ordered structure when obtained by thermal conversion of a solution-cast film of the precursor, with coherence lengths as determined from X-ray measurements of typically no more than 4 nm (ref. 7). If however, it is stretched as a free-standing film during the thermal conversion, very high degrees of alignment and crystallinity can be achieved[8,9]. For the photoisomer precursor we cannot obtain stretch-aligned films because thermal anchoring to a substrate is required to prevent overheating during the exothermic transformation reaction. For unoriented and disordered polyacetylene, where the lengths of the straight chain sequences are comparable to the characteristic width of the excited electronic states of the conjugated polymer (the soliton half-width, ξ, is of the order of $7a$ where a is the average carbon–carbon separation along the chain), we are always concerned to know the effects of disorder on the electronic structure and on the excited states of the π-electron system. We discuss the theoretical framework within which this can be modelled in the following section.

Electronic structure of disordered polyacetylene

The π-electron system of the *trans* isomer of polyacetylene can be considered as an example of a one-dimensional, half-filled electron band, with bond dimerization due to a Peierls distortion of the regular chain. Within the Peierls electron–phonon coupling model for the chain dimerization and π–π^* band gap, the gap ($2\Delta_0$) is determined by the dimensionless electron–phonon coupling constant, λ and a cut-off energy, E_c comparable to the bandwidth, $4t$ (where t is the intra-chain transfer integral), through the relation[10]

$$\Delta_0 = 2E_c \exp\{-1/2\lambda\} \qquad (1)$$

Using experimental values for the gap (1.9 eV) and the bandwidth (12 eV), the value of λ is required to be of the order of 0.2. This is rather larger than can be attributed to electron–phonon coupling alone, and it is widely held that the enhanced bond dimerization is due to the effects of the on-site Coulomb repulsion energy[11].

The modelling of polyacetylene in its excited states is usually performed using Hückel theory, with the various parameters (bandwidth, electron–phonon coupling, etc.) chosen empirically. This approach has been very successful, and we use it here for the modelling of the effects of disorder on the chain. The fundamental excitations of the half-filled band Peierls distorted chain are known to be phase kinks, or solitons, in the pattern of the bond alternation[12,13], with a gap parameter, Δ, which varies as $\Delta(x) = \Delta_0 \tanh(x/\xi)$, where $\xi = v_F/\Delta_0$ is the soliton half-width (estimated to be about $7a$) and v_F is the Fermi velocity.

The Raman-active models of *trans*-polyacetylene which modulate the degree of bond alternation (the amplitude modes of the soliton) are very sensitive to the local π electron structure on the chain, and large variations are seen for samples prepared by different routes, together with dispersion with photon energy, as seen for comparison of unoriented and stretch-oriented Durham polyacetylene[14]. Horovitz has shown that the frequencies of these modes are determined by the phonon response function

$$D_0(\omega) = \sum_n \frac{\lambda_n}{\lambda} \frac{\omega_n^{02}}{\omega_n^2 - \omega_n^{02}} = \frac{-1}{1-2\lambda} \qquad (2)$$

where λ_n/λ are the relative coupling parameters for the modes that couple to the bond dimerization ($n = 1$–3 for polyacetylene), ω_n^0 are the bare phonon frequencies for these modes[15,16], and λ is the effective electron–phonon coupling constant. The Raman frequencies obey the product rule

$$\prod_{n=1}^{3} \omega_n^2/\omega_n^{02} = 2\lambda \qquad (3)$$

This relation can be used when the energy gap can be treated using equation (1), with an empirically chosen value of λ, which can include some of the effects due to disorder, termed 'intrinsic' disorder by Horovitz *et al.*[15,16]. Vardeny *et al.*[17] include the effect of 'extrinsic' disorder, through a power series expansion of the bond-order condensation energy

$$E_i(\Delta) = E_0(\Delta) + b\Delta P \qquad (4)$$

where $E_0(\Delta)$ is the condensation energy in the defect-free system, keeping the lowest value of p that is non-vanishing. They have analysed data for the Raman dispersion of *trans* sequences in *cis*-rich Shirakawa polyacetylene, making the assumption that *trans* sequences are terminated by longer *cis* sequences, which have a preferred sense of bond alternation. They thus chose $p = 1$ in equation (4), since the extrinsic disorder (at the *trans* chain ends) breaks the inversion symmetry $\Delta \rightarrow -\Delta$. Their analysis gives

$$\ln(\Delta/\Delta_0) = bp\Delta^{p-2} \qquad (5)$$

and

$$\lambda/\lambda_0 = (2-p)\ln(\Delta/\Delta_0) + 1 \qquad (6)$$

where λ_0 is the effective coupling parameter without disorder and λ/λ_0 is related to the Raman frequencies through

$$\prod_{n=1}^{3} \omega_n^{s2}/\omega_n^{p2} = \lambda/\lambda_0 \qquad (7)$$

where ω_s are the Raman frequencies for the chains in the presence of disorder, and ω_p are the frequencies for the disorder-free chains. They have shown that variation of λ/λ_0 with laser excitation energy does follow the relation given by equation (6), with $p = 1$.

Turning to the nature of the disorder in unoriented films of Durham polyacetylene, and comparison with stretch-oriented Durham polyacetylene, we find that the band-gap in the unoriented material is raised, with the peak in the interband absorption raised from 1.9 to

2.3 eV[18–20], and we find concomitant increases in the frequencies of the Raman-active vibrational modes. In spite of the short lengths of straight chain however, the electronic excitations of the chain still have the character of the solitons, though the increased π–π^* gap affects these considerably[18–20]. We can model the effect of the conformational chain defects in the unoriented samples in a consistent way by using a value of the effective electron–phonon coupling constant, λ, that is some 8% higher than for the oriented samples. The use of λ as the principal parameter affected by disorder requires that the chain defects do not impose a preferred sense of bond alternation on the chains, so that it is possible to propagate a soliton through the chain defect. The 8% increase in the value of λ is measured directly from Raman scattering, using the product rule shown as equation (7), and taking values of ω_n for excitation at 647 nm for the two strongly dispersing modes ($n = 1$ and 3) of 1067 and 1461 cm^{-1} for the stretch-oriented samples and 1095 and 1473 cm^{-1} for the unoriented samples[14]. This increase in λ accounts for the increase in gap, $2\Delta_0$ from 1.9 to 2.3 eV through equation (1). This model has also been used to analyse the increased disorder found in Durham polyacetylene at the interface with silicon dioxide for the charge accumulation layer in MIS and MISFET structures[21].

RESULTS

Synthesis and molecular weight determination

The photoisomer precursor polymer was synthesized as previously described[5], though the synthesis was modified by the addition of a chain transfer agent, *trans* oct-4-ene, in the molar fractions listed in *Table 1* to regulate the molecular weight of the polymer. We have studied here the polymer prepared without any *trans* oct-4-ene present (long, or L sample), and with two different quantities of the chain transfer agent, medium, M, and short, S, as listed in *Table 1*.

Determinations of molecular weight were performed using gel permeation chromatography using tetrahydrofuran, THF, as eluent (Waters Associates model 590 programmable solvent delivery module and R401 differential refractometer, two Polymer Laboratories PL gel columns; 10^5 and 10^3 μm). Results for the L, M and S precursor polymers are given in *Table 1*. The expected trend in polymer chain length is observed, and consistent with this variation in molecular weight, we found that the L and M polymers formed good quality films when spin-coated from solution, though the S polymer produced poorer films which were non-uniform to the eye.

Film preparation

The polyacetylene precursors dissolved readily in butanone, and various solutions were made, ranging in concentration from 1 g of precursor in 10 ml butanone to 1 g precursor in 40 ml butanone. These solutions were very pale yellow in colour, indicating that very little conversion had taken place at room temperature. Films of the precursor were formed by spin coating onto an appropriate substrate (usually either Spectrosil glass or silicon) at speeds between 1600 rev min^{-1} and 2000 rev min^{-1}, depending on the thickness of film required. Thicker films were prepared by depositing drops of precursor solution onto the substrate, and allowing the solvent to evaporate. These procedures were carried out in a glove-box with oxygen and water levels of less than 5 ppm. The thermal conversion was carried out at a pressure of $< 10^{-5}$ Torr on a hotplate within an evaporator, which was situated inside a glove-box. For electrical characterization, metal contacts were also deposited within this evaporator, ensuring that the metal–polyacetylene interface was not exposed to even the trace amounts of oxygen and water present in the glove-box atmosphere.

In order to investigate the conditions required to convert the precursor to *trans*-polyacetylene, we fabricated structures consisting of a pair of closely spaced gold electrodes covered with a layer of precursor. The conductivities of these films were then measured as a function of time whilst the films were heated at various temperatures. *Figure 2* shows a plot of conductivity *versus* time for three identical samples of L polyacetylene, heated at 80, 100 and 120°C. It is apparent that the conductivity of the film heated at 80°C increases gradually, and reaches a maximum value of only 1.5×10^{-8} S cm^{-1}, whilst the films heated at 100 and 120°C both show sudden increases in conductivity after about 700 s, and reach maximum conductivities of around 3×10^{-6} S cm^{-1}. It is possible that the low conductivity of the 80°C sample is due to a relatively high concentration of *cis*-vinylene in the polyacetylene formed at this temperature, or to other chemical or conformational defects (see Discussion).

Figure 3 shows conductivity *versus* time graphs for samples of each of the three polyacetylenes converted at 100°C. This graph shows that the conductivity tends to increase as the chain length of the polymer decreases. This may arise from either a higher concentration of charge carriers or a higher carrier mobility in the shorter chain material. From these studies, we determined that preparation of polyacetylene films from these precursors was best performed at a temperature of between 100°C and 120°C, and these conditions were used for the rest of the work reported here.

Characterization by X-ray diffraction

X-ray diffraction measurements were performed using a Siemens single crystal AED diffractometer, with Ni

Table 1 Analysis by gel permeation chromatography of photoisomer precursors of differing degrees of polymerization

	Molar ratios						
	Monomer	WCl_6	$SnMe_4$	CT	M_n ($\times 10^3$)	M_w ($\times 10^3$)	M_w/M_n
Long, L	100	1	2	0	63	106	1.67
Medium, M	100	1	2	5	19	36	1.84
Short, S	100	1	2	10	15	26	1.75

CT is chain transfer agent, trans oct-4-ene. M_n and M_w are number and weight averages in polystyrene equivalents

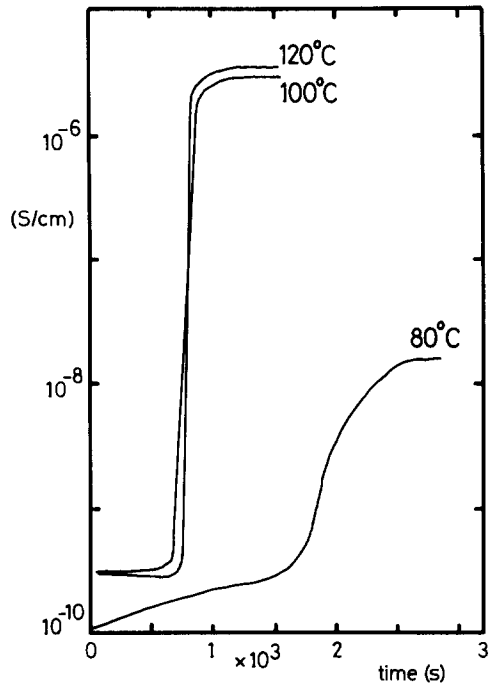

Figure 2 Variation with time of conductivity of the L precursor polymer during thermal conversion to polyacetylene at the temperatures indicated

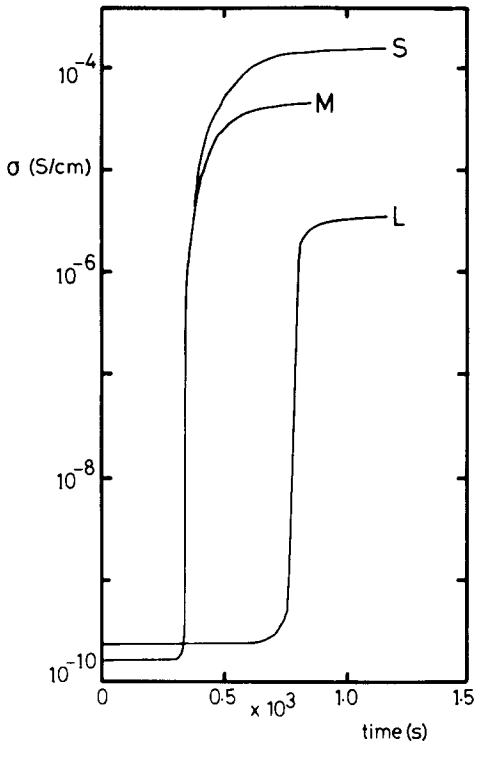

Figure 3 Conductivity *versus* time of heating at 100°C for the L, M and S precursor polymers

filtered CuKα radiation. We observe that there are very small differences between the materials prepared from the L, M and S photoisomer precursors, but that these materials are substantially more disordered than unoriented films of polyacetylene prepared by the standard Durham route[7]. A typical diffractometer scan is shown in *Figure 4*. The only diffraction peak seen is the (1 1 0), (2 0 0) reflection, which has a maximum at $2\theta = 24.2°$. This is similar to the value found for the standard Durham polyacetylene[7], and corresponds to an interchain spacing of 0.367 nm. The width, 2θ, of this peak can be used to obtain an estimate for the crystallite size, L, using the Scherrer formula, $L = K\lambda/\beta_{1/2} \cos\theta$, where K is usually taken to be 1, $\beta_{1/2}$ is the FWHM of the reflection, θ is the Bragg angle and λ is the wavelength of the X-rays (0.154 nm). The measured value of $\beta_{1/2}$ is 5°, after correction for instrumental broadening, and this gives a value for L of 1.8 nm. This value is considerably lower than found for unoriented films of polyacetylene prepared by the standard Durham route, for which values of 4.5 nm are found for films treated at 100°C[7]. The broad background can be attributed to that fraction of the sample which is non-crystalline. The ratio of this background to the peak intensity is much larger than observed for polyacetylene prepared by the standard Durham route, and together with the smaller crystallite size, indicates that the polyacetylene prepared from the photoisomer precursor is considerably more disordered than that obtained from the standard Durham precursor.

Infra-red spectroscopy

Infra-red (i.r.) spectra of the polyacetylene films were taken on a Nicolet 5SX-B FTIR spectrometer, using samples which were spin-coated onto KBr substrates. *Figure 5* shows spectra for films prepared from the L precursor converted at 100°C for 1 h (*Figure 5a*) and 4 h (*Figure 5b*). The intense bands found in the 1100–1300 cm^{-1} region after heating for 1 h are due to CF_3 groups in the residual precursor. These bands are much less intense in *Figure 5b*, indicating that heating for a longer period removes some of these species. It is interesting to note that the time required to remove the CF_3 is much longer than the time required to yield the maximum value of conductivity. Despite the fact that precursor polymer needs to be heated for only around 12 min to obtain a high conductivity, all films used for electrical characterization were heated for at least 2 h, in order to drive off as much of the CF_3-containing species as possible.

Infra-red spectra for films prepared from the L, M and S precursor polymers are shown in *Figure 6*. All three films were converted at a temperature of 100°C for 4 h; bands in the 1100–1300 cm^{-1} region indicate retention of fluorine. The main bands of interest are the intense *trans* C–H out-of-plane bending band at 1003 cm^{-1}, characteristic of polyacetylene, and the very weak equivalent *cis* C–H band at 717 cm^{-1} (ref. 22). The *cis*

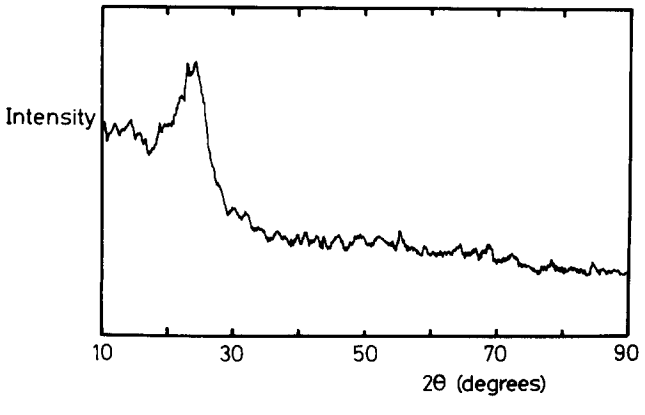

Figure 4 Diffractometer scan of a multilayer sample of polyacetylene prepared from the L precursor, obtained with CuKα X-rays ($\lambda = 0.154$ nm)

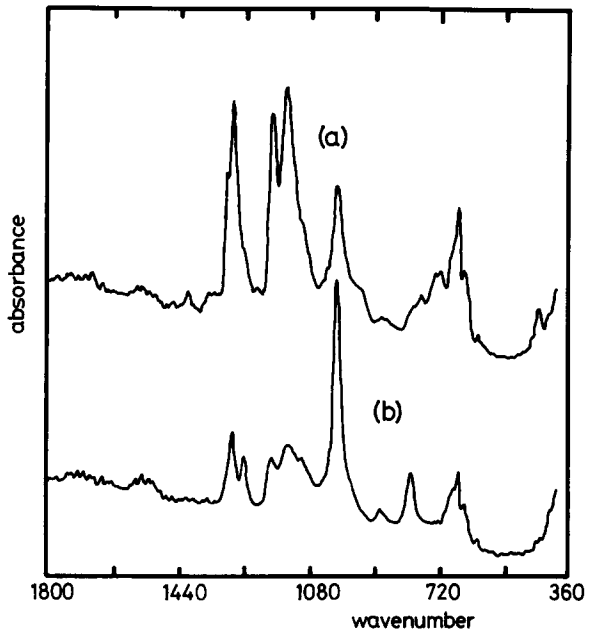

Figure 5 Infra-red absorption spectra of polyacetylene prepared from the L precursor, and converted at 100°C for (a) 1 h and (b) 4 h

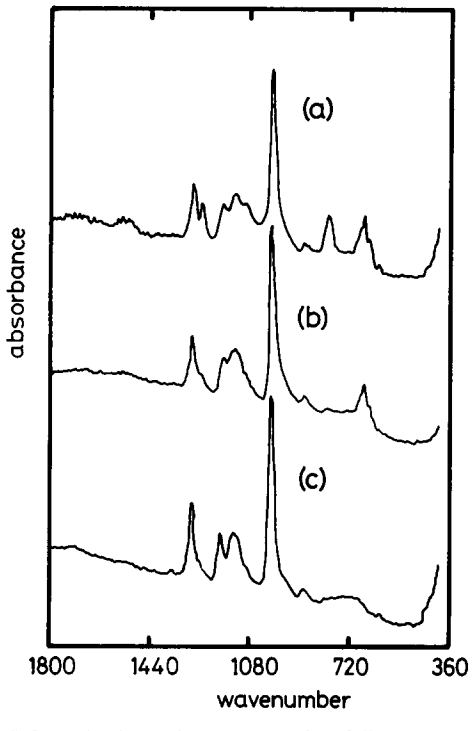

Figure 6 Infra-red absorption spectra for fully converted polyacetylene prepared from the L (a), M (b) and S (c) precursors

band is much weaker than that generally observed in conventional Durham-route polyacetylene, suggesting that *cis–trans* isomerization occurs much more rapidly and completely in the photoisomer precursor. This is not surprising, since the elimination reaction is expected to be very rapid and exothermic, due to the presence of the highly strained three- and four-membered rings in the photoisomer precursor. The heat evolved in this reaction may then drive the subsequent *cis–trans* isomerization process.

The three bands at 677, 666 and 649 cm^{-1} are not usually seen in the spectrum of polyacetylene, but have been observed here in spectra of all three chain length materials, and are also just discernible in spectra of the precursors. The origin of these bands remains uncertain.

X-ray and ultraviolet photoelectron spectroscopy

X-ray (X.p.s.) and ultraviolet photoelectron (u.p.s.) spectra were measured using a system described previously[23]. Thin films of the precursor polymer were spin-coated onto aluminium-coated substrates, and transferred to the UHV chamber for *in situ* thermal conversion and measurement. X-ray photoelectron spectroscopy is sensitive to the near-surface region of the sample, probing no more than 10 nm below the surface. The X.p.s. measurements show that there is some oxygen and a small amount of silicon in the samples examined; the aluminium substrate was not seen. The X.p.s. spectra for films measured before thermal conversion give an oxygen to carbon ratio of approximately 1:10, fluorine to carbon of 1:2, and silicon to carbon of 1:20. After thermal conversion, at 100°C for 4 h, the ratios were altered to oxygen to carbon 1:8, fluorine to carbon 2:11, and silicon to carbon 1:15. The silicon and oxygen present may be due to silicone grease, and the fall in the carbon to oxygen ratio after heating is most likely due to loss of hydrocarbon contamination from the surface. There is fluorine present in the sample after conversion; further heating was not found to decrease the fluorine content, and we consider that it is in the form of CF_3 groups attached directly to the conjugated polymer chain. The measured fluorine to carbon ratio gives about one pair of CF_3 groups per 30 carbon atoms on the chain. This value will represent a maximum fluorine content, since X.p.s. is sensitive to the surface layer (< 10 nm) and the low surface free energy of fluorocarbons will tend to cause the fluorinated residues to surface-segregate if there is sufficient mobility of the polymer chains during the conversion process.

Preliminary u.p.s. measurements were performed with HeI photons. The spectra obtained were slightly different than those obtained for polyacetylene prepared by the Shirakawa route[24]. In particular, we find a well-defined peak in the valence band spectrum at 5 eV binding energy (relative to the Fermi energy) which is not expected in the valence band for polyacetylene. This feature cannot be directly identified with features associated with the fluorine. It is possible however, that this structure is associated with the modified π-electronic structure in the vicinity of CF_3 side groups. Theoretical studies of this idea are in progress.

Optical absorption

Ultraviolet–visible–near infra-red spectra of films spin-coated onto Spectrosil glass substrates were recorded on a Perkin–Elmer Lambda 9 spectrophotometer. *Figure 7* shows the spectrum for a polyacetylene film prepared from the L precursor, very similar spectra were obtained for films prepared from the M and S precursors. We see from *Figure 7* that the band edge of the polyacetylene produced from the photoisomer precursor is at about 1.6 eV and the maximum of the π–π^* transition is at 2.65 eV. This value is higher than the 2.3 eV measured for standard unoriented Durham polyacetylene[18], as expected from the higher level of disorder.

Raman spectroscopy

Raman spectra were recorded with both a Dilors Omars 89 Instrument with a multidiode detector array

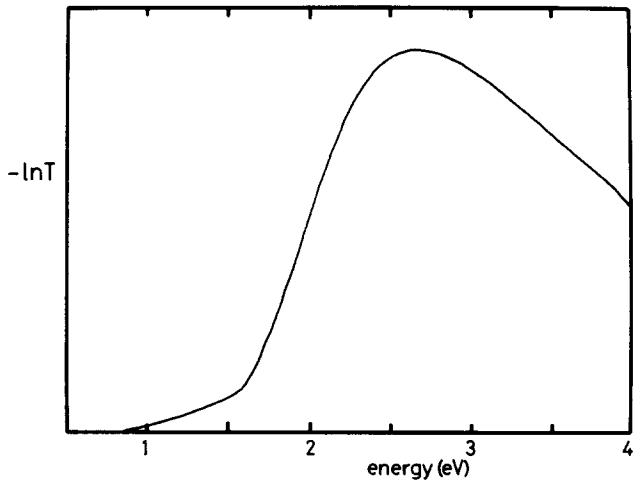

Figure 7 −Log(transmission) (optical absorbance) *versus* photon energy for a fully converted film of polyacetylene prepared from the L precursor

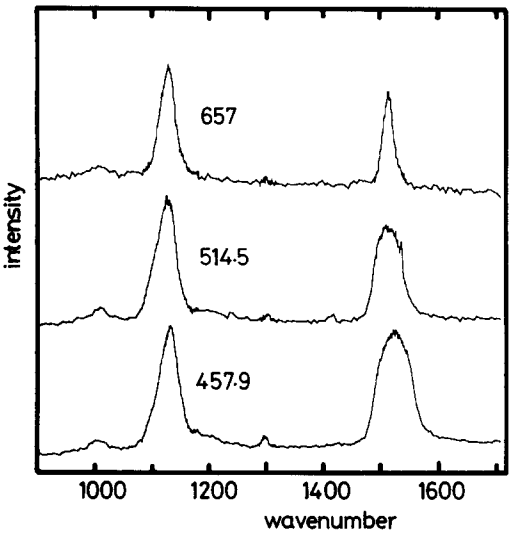

Figure 8 Raman spectra recorded at room temperature for polyacetylene prepared from the L precursor, measured at 457.9, 514.5 and 656 nm

and also with a modified Coderg Model PH1 double monochromator with Hamamatsu R943-02 photomultiplier tube. Excitation was provided by either an argon ion laser or a dye laser operating with R6G and DCM dyes. Spectra were recorded at room temperature. Typical spectra for polyacetylene from the L precursor are shown in *Figure 8* for excitation in the red, green and blue, and the energies for the peaks of these bands are given in *Table 2*. Frequencies for the two strongly dispersing modes are higher than observed in both the oriented and the unoriented standard Durham materials. There are some small differences between the spectra for the materials prepared from the L, M and S precursors, with lower frequencies measured for the M and S materials (*Table 2*). This indicates that the M and S materials possess better π conjugation along the chain, and therefore have better ordered structures.

As with all other forms of polyacetylene, there is strong dispersion of the modes with the energy of the exciting photons. This is generally agreed to arise from an inhomogeneous system, with a distribution of 'conjugation length' among the chains, and an associated distribution of π–π^* transition energies and frequencies of Raman-active vibrational modes. These modes are very strong when brought into resonance with the associated π–π^* transition, at 2Δ, and the effect of scanning the laser photon energy through the absorption band is to select a particular π–π^* transition and to measure the associated Raman frequencies for it. The relationship between the Raman frequencies and the effective coupling constant, λ is conveniently obtained from the product rule of Horovitz[15] given as equation (7). In this case, λ_0 is the limiting value of the coupling constant for 'long', defect-free chains, with frequencies ω_n^p, which we take here to be the case for excitation at 647.1 nm of the stretch-oriented material, and we can therefore plot a normalized value of λ against $\log(2\Delta)$. This is shown in *Figure 9* for the polyacetylene prepared from the L precursor, in which we also compare data for stretch-oriented and unoriented standard Durham route polyacetylene[14]. For this analysis only the two strongly

Table 2 Energies at the peaks in the two strongly dispersing Raman bands for polyacetylene prepared from the photoisomer precursors

	Long		Medium		Short	
Wavelength (nm)	$n=1$	$n=3$	$n=1$	$n=3$	$n=1$	$n=3$
457.9	1127	1516	1123	1507	1123	1503
	1130	1522[a]				
476	1129	1517[a]				
488	1125	1510	1120	1502	1118	1497
	1127	1513[a]				
514.5	1121	1505	1117	1493	1115	1493
	1122	1505[a]				
586	1109	1492[a]				
606	1107	1488[a]				
620	1109	1485	1107	1483	1107	1481
657	1099	1479	1101	1478	1102	1477

Data were recorded at room temperature, with a modified Coderg Model PH1 double monochromator, except where indicated[a], for which a Dilors Omars 89 Instrument with a multi-diode detector array was used

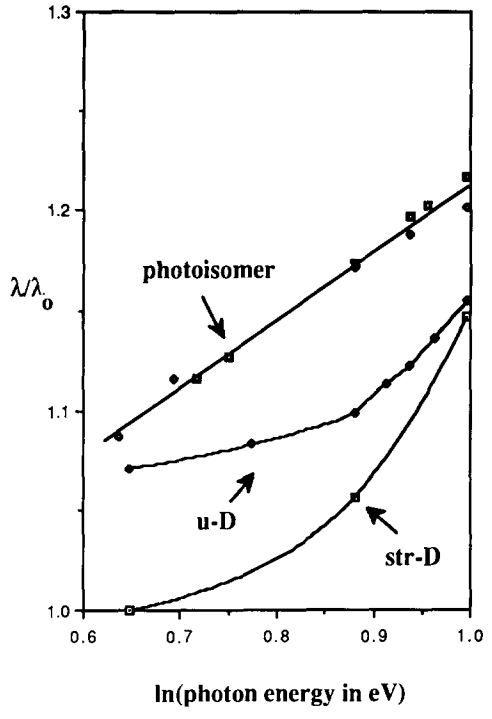

Figure 9 Dispersion of the effective electron–phonon coupling constant, λ, ratioed to the value of λ for 'long-chain' polyacetylene probed at low photon energies, determined through equation (3) from the data shown in *Table 2*. Data shown are for the polymer prepared from the L precursor, and also for stretch-oriented (str-D) and unoriented (u-D) standard Durham polyacetylene[14]

dispersing modes ($n = 1$ and 3) were used as input to the product rule.

The work of Horovitz *et al.* establishes that there is no single correspondence between λ and 2Δ (refs 15 and 16). The relation between the two depends on the nature of the disorder that is present, ranging from a very weak dispersion if the defects do not impose a preferred sense of bond alternation ($p = 2$ in equations (4)–(6)), to a very strong dispersion if the defects break this symmetry, with a gradient of 1 in the plot of λ/λ_0 *versus* $\ln(2\Delta)$. This latter limit is observed for *trans* in *cis*-rich polyacetylene prepared by the Shirakawa route[17]. We have previously argued that disorder in unoriented standard polyacetylene is of the '$p = 2$' type, and that its effect on the Raman frequencies, band gap, soliton width, soliton effective mass and soliton-to-band optical cross-section can be parametrized through an increased value of λ[13,18–21]. For the polyacetylene prepared by the photoisomer route it is clear that there is increased disorder, with energies of both the electronic and vibrational excitations of the chain raised. The plot of λ/λ_0 *versus* $\ln(2\Delta)$ in *Figure 9* shows an apparently linear variation of λ/λ_0 with $\ln(2\Delta)$, but the gradient is 0.34, very much lower than the value of 1 expected for '$p = 1$' defects through equation (6).

Detailed interpretation of the Raman dispersion must take into account the variation of scattering intensity with excitation energy. We do not have accurate values for this here, but we have observed that the scattering intensity for excitation in the red is lower than that for excitation in the green and blue, and we consider that this is consistent with the fact that the median value for the π–π^* transition, at the peak in the absorption band, is at 2.65 eV, and that there is therefore only a small proportion of the material in resonance below this energy.

To compare the values of λ and 2Δ we take the value of λ/λ_0 at the peak of the optical absorption spectrum, i.e. $\lambda/\lambda_0 = 1$ at 1.95 eV and $\lambda/\lambda_0 = 1.08$ at 2.3 eV for the stretch-oriented and unoriented standard Durham materials, respectively, and $\lambda/\lambda_0 = 1.15$ at 2.65 eV for the material prepared from the photoisomer precursor. Fitting equation (1) with reasonable values for E_c (6 eV) and λ (0.2) to match the experimental value of $2\Delta = 1.9$ eV for the 'long' chain polyacetylene, we can use the measured values of λ/λ_0 to derive values of $2\Delta = 2.4$ eV for the unoriented standard Durham polyacetylene, and $2\Delta = 2.7$ eV for the polyacetylene prepared from the photoisomer precursor. The agreement between these and the experimental values is good, and we consider that this is evidence that the effects of disorder in polyacetylene are similar to, though stronger than, those in polyacetylene prepared by the standard Durham route, and can be modelled with an increased value of the electron–phonon coupling constant.

Electrical conductivity

In-plane direct current conductivity measurements were performed on devices consisting of two closely spaced gold electrodes coated with a layer of polyacetylene. Temperature-dependent measurements of conductivity were performed in a continuous flow helium cryostat, with sample transfer arranged to avoid exposure to air. Conductivities were measured using a Keithley 617 electrometer.

Room temperature conductivities are shown in *Table 3*. *Figure 10* shows the conductivity of polyacetylene prepared from the L, M and S photoisomer precursors, plotted against reciprocal temperature. Over this temperature range (225–300 K) the variation of conductivity with temperature is activated with an energy of activation of about 0.5 eV for the L and M materials, and about

Table 3 Transport data for polyacetylene prepared from the L, M and S photoisomer precursors

	Conductivity at 300 K ($S\,cm^{-1}$)	Activation energy (eV)	Acceptor concentration (cm^{-3})	Mobility ($cm^2\,V^{-1}\,s^{-1}$)
L	3.3×10^{-8}	0.5	3.0×10^{17}	0.7×10^{-6}
M	5.5×10^{-8}	0.5	2.0×10^{16}	1.7×10^{-6}
S	3.3×10^{-7}	0.4	1.5×10^{16}	1.3×10^{-5}

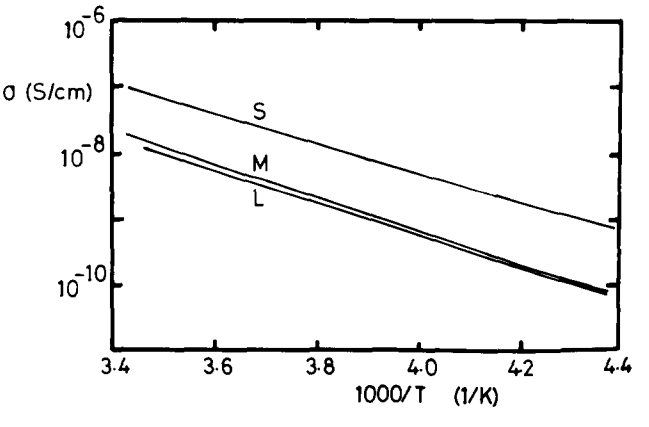

Figure 10 Conductivity of polyacetylene prepared from the L, M and S photoisomer precursors plotted against reciprocal temperature

0.4 eV for the S material. These values for the activation energy are a little higher than those of stretch-oriented and unoriented standard Durham polyacetylene, for which values lie in the range 0.35–0.4 eV[25]. As for these materials, we consider that the activation energy is due to an activated carrier mobility rather than a thermally activated population of carriers.

Properties of metal–insulator–semiconductor structure

A convenient method for determining extrinsic majority carrier concentration in a semiconductor is to measure the depletion layer capacitance of the Schottky barrier or metal–insulator–semiconductor (MIS) diode formed from the semiconductor[2,21]. The MIS diodes are easier to fabricate than Schottky diodes, since the insulator layer provides a barrier against short-circuits through the semiconductor due to, for example, pin-holes. For this study we used structures of the type previously used with the standard Durham polyacetylene[2,21]. We used a silicon substrate n-doped to form a highly conducting surface layer of thickness 400 nm, onto which was grown a silicon dioxide layer which acts as the insulator layer. The polyacetylene layer was then formed by spin-coating the precursor polymer and thermally converting to polyacetylene, and this was capped with a thin layer of gold, deposited by evaporation, which forms the ohmic top contact. All sample preparation involving the polyacetylene was performed inside a glove box containing a dry and oxygen-free (<5 ppm) argon atmosphere. Capacitance *versus* applied voltage measurements were performed using a Hewlett-Packard 4192A impedance analyser interfaced to a Hewlett-Packard microcomputer.

The MIS structure allows the possibility of band bending at the insulator–semiconductor interface through the Fermi level to produce a surface charge layer which may be the same carrier sign as the majority carriers (accumulation layer) or as the minority carriers (inversion layer)[26]. The formation of accumulation, depletion and inversion layers may be demonstrated through the behaviour of the device capacitance with respect to the bias voltage. The measured capacitance, C, is that of the series combination of the insulator capacitance, C_i, and the capacitance of the active region of the semiconductor, C_d, and is given by $C = C_i C_d/(C_i + C_d)$. Since C_d is large for the accumulation and inversion layers, C is equal to the geometric capacitance of the insulating layer, but C falls to a lower value for movement of the depletion layer. The variation of C with bias voltage in the depletion regime has been modelled by Goetzberger and Nicollian[27] for the case of a p-type semiconductor as

$$\left(\frac{C_i}{C}\right)^2 - 1 = \left(\frac{C_i}{A}\right)^2 \frac{2(V - V_f)}{qN_A\varepsilon_r\varepsilon_0} \qquad (8)$$

where A is the device area, ε_r the relative dielectric constant of the semiconductor (taken here to be 2.75), N_A the acceptor concentration and V_f the flat-band voltage.

The capacitance *versus* bias voltage curve for an MIS structure with polyacetylene formed from the L precursor is shown in *Figure 11* as $(C_i/C)^2$ *versus* bias voltage, V, and illustrates that this device functions in a very similar way to the standard Durham polyacetylene MIS devices[2,21]. We find as expected that the extrinsic charge carriers are positive, and that the capacitance for negative gate voltages flattens out to the geometric capacitance

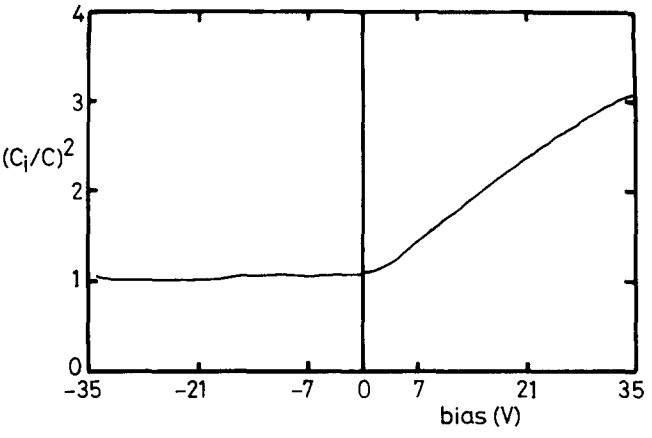

Figure 11 Capacitance, C, of a polyacetylene MIS structure formed from the L photoisomer, plotted as $(C_i/C)^2$ *versus* bias voltage. The measurements were performed at 70 Hz

of the insulator, indicating the formation of an accumulation layer. The decrease in the measured capacitance for positive voltages displays the formation of the depletion layer. Saturation of the capacitance for large positive biases sets in when the depletion layer extends across the polyacetylene film and is not observed for this device. Inversion layer formation for these MIS structures is not seen at high positive biases; the usual problem for the two-terminal device is that the mechanism for the generation of minority carriers is through the thermal generation of electron-hole pairs at the interface region, and transport of the majority carriers through the bulk of the semiconductor to the back contact. This is usually limited by the thermal generation rate, which in the case of an anisotropic semiconductor such as polyacetylene is further impeded[19] by the difficulty of achieving charge separation for a system showing predominantly one-dimensional diffusion.

The results in *Figure 11* show a constant gradient of $(C_i/C)^2$ *versus* V in the depletion regime, and analysis of the slope using equation (8) gives a value for the concentration of extrinsic carriers. This is found to be about 3.0×10^{17} cm^{-3}, within the range found for the standard Durham material[2,21]. The C–V characteristics of devices made with the M and S precursors are qualitatively similar and values for N_A are shown in *Table 3*. Carrier mobilities calculated from the room temperature conductivities and the values of N_A are also shown in *Table 3*. The values of N_A for these polymers all lie within the range observed for the standard Durham polyacetylene, and we consider that the origin of these carriers is the same for materials prepared by the two routes. We have previously suggested that they may be associated with metathesis catalysts left at the ends of the polymer chain after polymerization of the monomer using conventional $WCl_6/(CH_3)_4Sn$ based initiation, and we would expect this to be similar for both classes of precursor.

We note that the mobility of the charge carriers in the polymer tends to increase as the chains become shorter, though all these mobility values are low compared to those found for the standard Durham material. A similar effect has been observed in polythiophene oligomers[28], and has been interpreted in terms of improved ordering of the polymer chains as they become shorter. There is some evidence for better order in the polyacetylene prepared from the S and M precursors from the

frequencies of the Raman modes collected in *Table 2*; these are consistently a couple of wavenumbers lower than for the samples prepared from the L precursor. However, these differences are small, and we have not been able to find corroborating trends in the X-ray data.

DISCUSSION

We find from the range of measurements reported here that polyacetylene prepared by the photoisomer route can be conveniently handled in the form of thin films cast on substrates; the precursor polymer is stable at room temperature and the exothermic elimination reaction can be controlled if the film is well anchored thermally. However, the polyacetylene formed by this route has the disadvantage that the structure is considerably more disordered than that formed from the standard Durham precursor polymer. As we discuss below, this is probably associated with the residual fluorine in the converted polymer.

Both i.r. and X.p.s. measurements provide convincing evidence that even thin films of polyacetylene prepared from the photoisomer precursor retain fluorine in the final polymer, whereas fluorine is essentially absent from polyacetylene films prepared from the triene precursor polymer. This observation can be rationalized in terms of possible mechanisms for conversion of precursor polymers to polyacetylene. Thus, for the conventional precursor polymer the elimination of hexafluoroxylene is a symmetry-allowed thermal process[29]; by contrast, the loss of hexafluoroxylene from the photoisomer precursor polymer requires that two cyclopropyl carbon–carbon bonds are broken to generate the triene precursor which then eliminates the aromatic unit, shown as route 1 in *Figure 12*. However, bond breaking in the strained polycyclic units of the photoisomer precursor polymer may occur via other routes; two are indicated in *Figure 12*. There is some experimental evidence that can be cited in support of such a hypothesis in as much as it is known that trifluoromethylcyclopropane undergoes a thermal ring opening by breaking of the carbon–carbon bonds either adjacent to or opposite the site of substitution[30]. If we consider the processes which could follow an initial cyclopropyl bond breaking we have, in addition to the route which leads to polyacetylene, two pathways (routes 2 and 3) which lead to polyenes in which trifluoromethyl groups are retained. These alternative routes are inherently less likely on grounds of the steric constraints which have to be overcome and the requirement for nearly simultaneous breaking of three bonds rather than the two of route 1, but they may occur with sufficient frequency to account for the observed retention of fluorine.

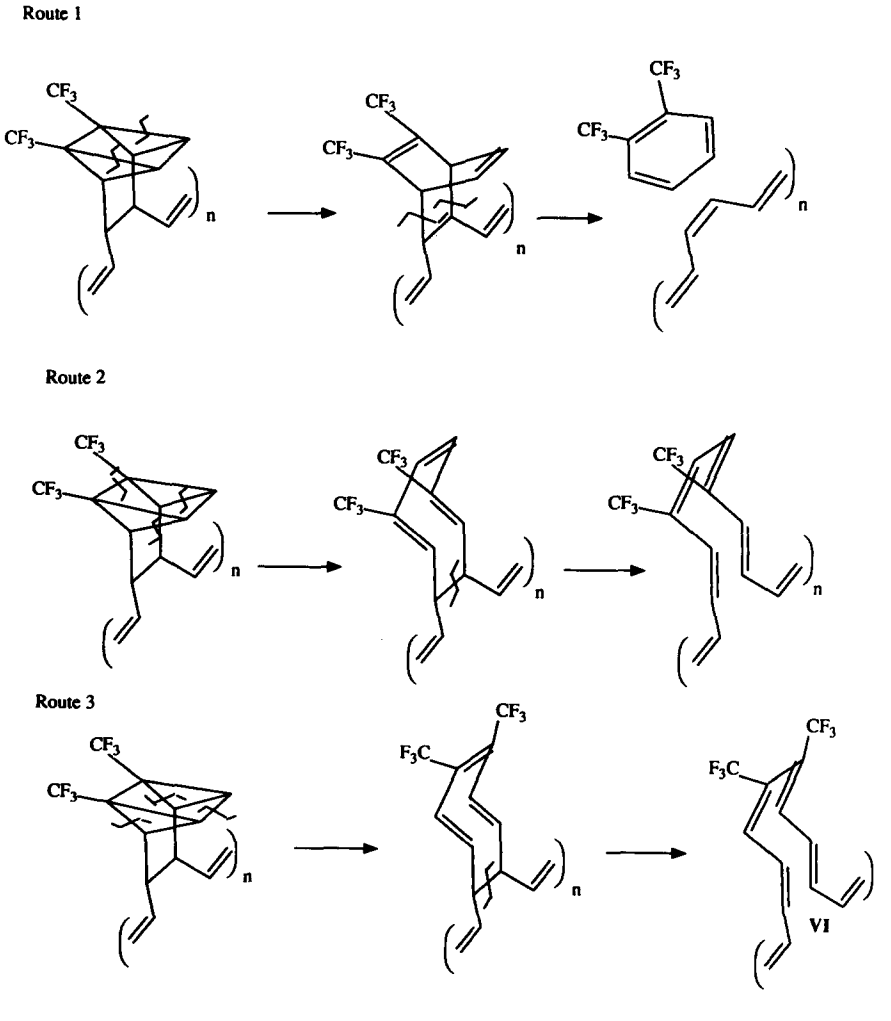

Figure 12 Schemes for thermal conversion of the photoisomer, showing (1) elimination of cyclofluoroxylene to yield polyacetylene, and (2), (3) retention of the trifluoromethyl groups on the polymer chain

The presence of these side groups is very likely to be responsible for the greater disorder observed in the polyacetylene samples prepared by the photoisomer route as compared to those produced with the normal precursor. Thus, considerable relaxation of the polymer chain would be required in the regions where the trifluoromethyl groups are retained if a very contorted polyene conformation is to be avoided, and such relaxations may not be possible in this system. Further, in route 3, a polyene sequence with two adjacent trifluoromethyl groups is postulated, and this requires that the vinylenes involved adopt a perpendicular conformation[31].

The effect of chain disorder and defects on the electronic and vibrational structure of the chains is an important issue for all experimental studies of this polymer, and we have used here the model we have previously used to describe disorder in polyacetylene prepared by the standard Durham precursor route. The effects of disorder are lumped into an effective electron–phonon coupling constant, λ, and the electronic and vibrational structure are consistently described. This model has the important quality of preserving the formal description of the coupled π-electron lattice system as a Peierls-distorted dimerized chain. Thus, in spite of the disorder present, the soliton-like character of the electronic excitations of the chain is retained, as we have demonstrated when charge is introduced onto the chain by chemical doping, photoexcitation and charge injection in device structures for polyacetylene prepared by the standard Durham route[18–21]. Similar experiments with the photoisomer-derived polymer are planned.

ACKNOWLEDGEMENT

It is a pleasure to thank J. H. Burroughes and E. A. Marseglia for their assistance with this work.

REFERENCES

1 Edwards, J. H. and Feast, W. J. *Polym. Commun.* 1980, **21**, 595
2 Burroughes, J. H., Jones, C. A. and Friend, R. H. *Nature* 1988, **335**, 136
3 Bott, D. C., Brown, C. S., Chai, C. K., Walker, N. S., Feast, W. J., Foot, P. J. S., Calvert, P. D., Billingham, N. C. and Friend, R. H. *Synth. Met.* 1986, **14**, 245
4 Foot, P. J. S., Calvert, P. D., Billingham, N. C., Brown, C. S., Walker, N. S. and James, D. I. *Polymer* 1986, **27**, 488
5 Feast, W. J. and Winter, J. N. *J. Chem. Soc. Chem. Commun.* 1985, 202
6 Feast, W. J., Parker, D., Winter, J. N., Bott, D. C. and Walker, N. S. *Springer Ser. Solid State Sci.* 1985, **63**, 45
7 Brown, C. S., Vickers, M. E., Foot, P. J. S., Billingham, N. C. and Calvert, P. D. *Polymer* 1986, **27**, 1719
8 Leising, G. and Kahlert, H. *Mol. Cryst. Liq. Cryst.* 1985, **117**, 1
9 Sokolowski, M., Marseglia, E. A. and Friend, R. H. *Polymer* 1986, **27**, 1714
10 Takayama, H., Lin-Liu, Y. R. and Maki, K. *Phys. Rev.* 1980, **B21**, 2388
11 Baeriswyl, D. and Maki, K. *Phys. Rev.* 1985, **B31**, 6633
12 Su, W. P., Schrieffer, J. R. and Heeger, A. J. *Phys. Rev. Lett.* 1979, **42**, 1698; *Phys. Rev.* 1980, **B22**, 2099; 1983, **B28**, 1138
13 Rice, M. J. *Phys. Lett.* 1979, **71A**, 152
14 Friend, R. H., Bradley, D. D. C., Pereira, C. M., Townsend, P. D., Bott, D. C. and Williams, K. P. J. *Synth. Met.* 1986, **13**, 101
15 Horovitz, B. *Solid State Commun.* 1982, **41**, 729
16 Ehrenfreund, E., Vardeny, Z., Brafman, O. and Horovitz, B. *Phys. Rev.* 1987, **B36**, 1535
17 Vardeny, Z., Ehrenfreund, E., Brafman, O. and Horovitz, B. *Phys. Rev. Lett.* 1985, **54**, 75
18 Friend, R. H., Bradley, D. D. C., Townsend, P. D. and Bott, D. C. *Synth. Met.* 1987, **17**, 267
19 Friend, R. H., Bradley, D. D. C. and Townsend, P. D. *J. Phys.* 1987, **D20**, 1367
20 Friend, R. H., Schaffer, H. E. and Heeger, A. J. *J. Phys.* 1987, **C20**, 6013
21 Burroughes, J. H., Jones, C. A., Lawrence, R. A. and Friend, R. H. Proceedings on NATO ARW on 'Applications of Conjugated Polymers', Mons, Belgium, September 1989
22 Fincher, C. R., Ozaki, M., Heeger, A. J. and MacDiarmid, A. J. *Phys. Rev.* 1979, **B19**, 4140
23 Salaneck, W. R., Bergman, R., Sundgren, J.-E., Rockett, A. and Greene, J. E. *Surf. Sci.* 1988, **198**, 461
24 Lögdlund, M., Salaneck, W. R., Stafström, S., Bradley, D. D. C., Friend, R. H., Ziemelis, K. E., Froyer, G., Swanson, D., MacDiarmid, A. G., Lazzaroni, R., Meyers, F. and Brédas, J.-L. *Synth. Met.* in press
25 Townsend, P. D. and Friend, R. H. *Phys. Rev.* 1989, **B40**, 3112
26 Sze, S. M. 'Physics of Semiconductor Devices', 2nd Edn, Wiley Interscience, New York, 1981
27 Goetzberger, A. and Nicollian, E. H. *Appl. Phys. Lett.* 1966, **9**, 12
28 Fichou, D., Horovitz, G., Nishikitani, Y. and Garnier, F. *Synth. Met.* 1989, **28**, C723
29 Bott, D. C., Brown, C. S., Edwards, J. H., Feast, W. J., Parker, D. and Winter, J. N. *Mol. Cryst. Liq. Cryst.* 1985, **117**, 9
30 Placzek, D. W. and Rabinovitch, B. S. *J. Phys. Chem.* 1965, **69**, 2141
31 Chambers, R. D., Clark, D. T., Kilcast, D. and Partington, S. *J. Polym. Sci., Polym. Chem. Edn* 1974, **12**, 1647